Crystal Structure of the Ternary Complex of Ribulose-1,5-bisphosphate Carboxylase, Mg(II), and Activator CO_2 at 2.3-Å Resolution†,‡

Tomas Lundqvist and Gunter Schneider*

Department of Molecular Biology, Swedish University of Agricultural Sciences, Uppsala Biomedical Center, Box 590, S- 751 24 Uppsala, Sweden

Received June 15, 1990; Revised Manuscript Received October 9, 1990

ABSTRACT: The activated ternary complex, enzyme–CO_2–Mg(II), of the dimeric ribulose-1,5-bisphosphate carboxylase/oxygenase from *Rhodospirillum rubrum* can be prepared in the same crystal form that was used for the crystallographic structure determination of the native nonactivated enzyme [Schneider, G., Bränden, C.-I., & Lorimer, G. (1986) *J. Mol. Biol. 187*, 141–143). The three-dimensional structure of the activated enzyme has been determined to a nominal resolution of 2.3 Å by protein crystallographic methods. The activator CO_2 forms a carbamate with Lys191, located at the bottom of the funnel-shaped active site. In both subunits, this labile adduct is stabilized by a Mg(II) ion, bound to the carbamate and the side chains of Asp193 and Glu194. One solvent molecule was found within the first coordination sphere of the metal ion. The metal-binding site in ribulose-1,5-bisphosphate carboxylase consists thus of at least three protein ligands, all located on loop 2 of the β/α barrel. One additional metal ligand, the side chain of the conserved Asn111, was observed close to the Mg(II) ion in the B-subunit. Other structural differences at the active site between the activated and nonactivated enzyme are limited to side-chain positions. Nevertheless, it is obvious that the hydrogen-bonding pattern in the vicinity of the activator site is completely altered.

Green plants use most of the chemical energy trapped by the light reaction of photosynthesis to drive the fixation of carbon dioxide. This process takes place in the stroma of chloroplasts through an ingenious cycle of reactions generally referred to as the Calvin cycle. It is the only known way by which carbon dioxide can be brought into the biosphere in significant amounts. In the initial reaction of the Calvin cycle, one molecule of CO_2 is added to ribulose-1,5-bisphosphate to yield two molecules of 3-phosphoglycerate through the action of ribulose-1,5-bisphosphate carboxylase/oxygenase (EC 4.1.1.39, RuBP-carboxylase).[1] This results in the net fixation of one carbon that can be used in anabolic processes. However, in a competing reaction the same enzyme also catalyzes an oxygenase reaction where, after the addition of an O_2 molecule, ribulose-1,5-bisphosphate splits into one molecule of phosphoglycerate and one of phosphoglycolate. The latter molecule is shunted into the glycolate pathway. The only apparent function of the glycolate pathway is to salvage as much as possible of the energy otherwise lost through the oxygenase reaction. It has been shown that this process, called photorespiration, is a major limitation to crop production (Hardy et al., 1978). A deeper understanding of photorespiration, with the eventual aim of minimizing its effect, is thus desirable.

Two forms of RuBP-carboxylase are found. In higher plants, algae, and most other photosynthetic organisms, the enzyme is a complex molecule consisting of eight large and eight small subunits, forming an L_8S_8 complex. In the photosynthetic bacterium *Rhodospirillum rubrum*, the enzyme is a dimer of large subunits, L_2 [for a recent review see Andrews and Lorimer (1987)]. The three-dimensional structures of the L_2 form (Schneider et al., 1986b, 1990a) and two L_8S_8-type RuBP-carboxylases, from spinach (Anderson et al., 1989; Knight et al., 1989) and tobacco (Chapman et al., 1987, 1988), have been determined. The L-subunit, which carries the catalytic function, is very similar in structure despite the low overall homology between the L_2 and the L_8S_8-type RuBP-carboxylases (approximately 25%). Two domains make up the large subunit. The active site is located at the carboxy end of the β/α barrel of the C-terminal domain (Schneider et al., 1986b). Residues from the N-terminal domain of the second subunit complete the active site, which is built up from two subunits. Consequently, the L_2 unit is the minimal functional building block of the enzyme, with two active sites at the interface between subunits (Schneider et al., 1986b; Larimer et al., 1987).

Activation by the formation of a ternary enzyme–CO_2–Mg(II) complex (Figure 1) is common to all RuBP-carboxylases irrespective of their origins and composition (Andrews & Lorimer, 1987). The site of activation is the ϵ-amino group of Lys191, which slowly reacts with a molecule of CO_2 to form a carbamate (Lorimer & Miziorko, 1980; Lorimer, 1981). The activating CO_2 is distinct from the substrate CO_2 molecule. Rapid binding of a divalent metal ion stabilizes the labile carbamate to form the active ternary complex (Lorimer, 1979).

An increasing number of experiments shows that the metal ion is essential for the catalytic reaction. The *R. rubrum* enzyme shows catalytic activity with a number of divalent metal ions: Mg(II), Mn(II), Fe(II), Co(II), or Cu(II) (Christeller, 1981; Robison et al., 1979; Bränden et al., 1984; Pierce & Reddy, 1986). With Co(II) only the oxygenase reaction is observed (Robinson et al., 1979; Christeller, 1981). The importance of Lys191 for catalytic activity has been

† This work has been supported by grants from the Swedish Natural Science Research Council and E. I. du Pont de Nemours and Co., Inc., Wilmington, DE.

‡ The atomic coordinates of the ternary complex have been submitted to the Brookhaven Protein Data Bank.

[1] RuBP-carboxylase, ribulose-1,5-bisphosphate carboxylase/oxygenase; 2-CABP, 2-carboxyarabinitol-1,5-bisphosphate; MPD, 2-methyl-2,4-pentanediol; TNBS, trinitrobenzenesulfonate; F_o, observed structure factor amplitude; F_c, calculated structure factor amplitude.

0006-2960/91/0430-904$02.50/0

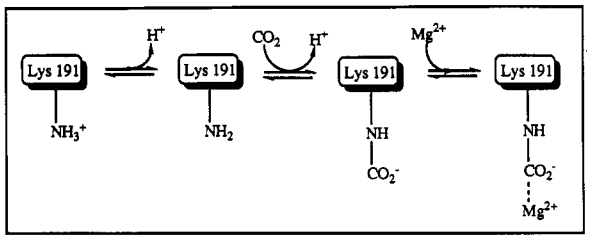

FIGURE 1: Activation of RuBP-carboxylase.

verified by site-directed mutagenesis. The replacement of this side chain by a glutamic acid side chain (Estelle et al., 1985) resulted in an enzyme devoid of oxygenase and carboxylase activity. On the basis of model-building experiments using the atomic model of RuBP-carboxylase from *R. rubrum* (Schneider et al., 1986b, 1990a), two conserved acidic side chains, Asp193 and Glu194 were implicated to be part of the metal-binding site. Subsequent site-directed mutagenesis of these two residues (Lorimer et al., 1987) revealed that none of the mutants sustained catalysis. The proposed role of the metal in polarizing the carbonyl group at C-2 of the substrate and thereby facilitating the enolization reaction (Andrews & Lorimer, 1987) is supported by the fact that none of these mutants shows exchange of the C-3 hydrogen of the substrate with bulk solvent. The proper metal coordination thus seems to be a necessary requirement for the enolization of the substrate, ribulose-1,5-bisphosphate. Even with the modest change from an aspartic acid side chain to the corresponding amide, enolization is abolished. Direct interaction between the metal and the reaction intermediate analogue 2-CABP has been shown both by ^{13}C nuclear magnetic resonance (Pierce & Reddy, 1986) and crystallographic studies (Andersson et al., 1989). Thus, a complete description of the environment around the metal, during different stages of catalysis, is crucial to our understanding of this enzyme and its mechanism of action. In the following we describe the results of the crystal structure analysis of activated RuBP-carboxylase from *R. rubrum* at 2.3-Å resolution.

Materials and Methods

Recombinant RuBP-carboxylase from *R. rubrum* (Sommerville & Sommerville, 1984; Pierce & Gutteridge, 1985) with an additional 24 amino acids from β-galactosidase at the N-terminus (Nargang et al., 1984) was crystallized under nonactivating conditions as described in Schneider et al. (1986a). The crystals are monoclinic, $P2_1$, with cell dimensions a = 65.5 Å, b = 70.6 Å, c = 104.1 Å, and β = 92.1°. Crystals were obtained by dialyzing the enzyme solution against 2-(*N*-morpholino)ethanesulfonic acid buffer at pH 5.6, the isoelectric point of the enzyme. In order to raise the pH to a value more favorable for carbamate formation, crystals were gradually transferred to a solution containing 50% 2-methyl-2,4-pentanediol (MPD) by increasing the MPD concentration stepwise by 5% at 4 °C. After the MPD additions, the crystals were dialyzed against a buffer solution of pH 8.1, containing 50 mM $MgCl_2$ and 25 mM $NaHCO_3$ for 1 day.

Diffraction data to a resolution of 2.3 Å were collected on a Nicolet Xentronics area detector (Durbin et al., 1986) using the software described by Blum et al. (1987). Data handling and data processing were done with the program PROTEIN (Steigemann, 1974). Data collection statistics are given in Table I and Figure 2. Electron density maps with coefficients $|F_o| - |F_c|$ and $2|F_o| - |F_c|$ were computed. The phase angles used initially were derived from a model of the native deactivated protein, which had a crystallographic *R*-factor [$R = (\Sigma|F_o - F_c|/\Sigma|F_o|) \times 100$] of 18.0% at 1.7-Å resolution

Table I: Data Collection Statistics[a]

	no. of measurements	no. unique	*R*-merge[b]	% of total
crystal 1	32313	24009	4.32	56.1
crystal 2	58785	30651	5.34	69.5
total	91098	38794	6.06	87.9

[a] Intensity data of the ternary complex of RuBP-carboxylase with Mg(II) and activator CO_2 were collected to 2.3-Å resolution. [b] *R*-merge = $[\sum^N\sum^n(I - \langle I\rangle)/\sum^N n\langle I\rangle] \times 100$, where N is the number of unique measurements, n is the number of multiple measurements of a particular reflection, I is the measured intensity, and $\langle I\rangle$ is the mean intensity of a reflection.

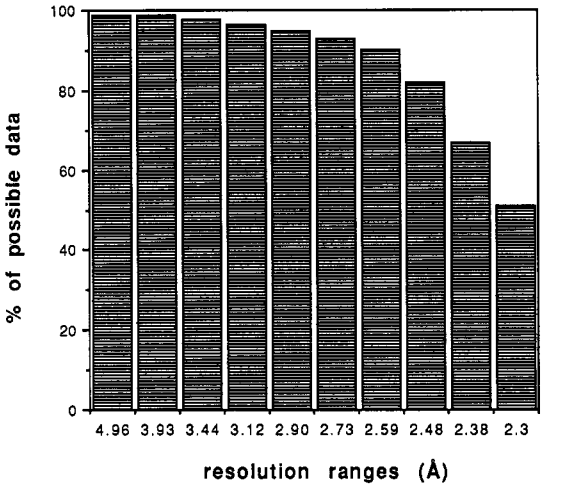

FIGURE 2: Completeness of the measured intensity data as a function of the resolution.

(Schneider et al., 1990a). An Evans and Sutherland PS330 running FRODO (Jones, 1978, 1982) was used to inspect the model and manually correct errors.

The initial model was refined by simulated annealing using the program XPLOR (Brünger et al., 1987). A molecular dynamic simulation was run for 0.75 ps at 2000 K with a time step of 0.5 fs. The temperature was raised to 4000 K, and the structure was subsequently slowly cooled to 300 K by using a 25 K temperature drop every 50 dynamics steps of 0.5 fs. Subsequent energy minimization and refinement of atomic temperature factors gave an *R*-value of 16.9% for all reflections between 10 and 2.5 Å. Final refinement, to 2.3-Å resolution, was achieved by using least-squares methods with the FFT version of PROLSQ (Konnert & Hendrickson, 1980) contained in the CCP4 program package (Daresbury, England). After 50 cycles of refinement, the final model had an *R*-factor of 19.3% for all reflections between 5.5 and 2.3 Å. The higher *R*-value obtained after the PROLSQ refinement is partly due to the fact that the refinement with XPLOR minimized the *R*-factor at the expense of reasonable stereochemistry. The final model has good stereochemistry as indicated by the root-mean-square deviation for bond lengths of 0.013 Å and for bond angles of 2.1°. Superposition of the two subunits of the *R. rubrum* enzyme and the L-subunits of the spinach RuBP-carboxylase was done by least-squares methods using the program O (Jones et al., 1990).

Results

The model of the activated RuBP-carboxylase, E–CO_2–Mg(II), has been refined to a nominal resolution of 2.3 Å, resulting in a final model with a crystallographic *R*-value of 19.3% for all reflections between 5.5 and 2.3 Å. Initial phases were derived from the structure of the nonactivated enzyme,

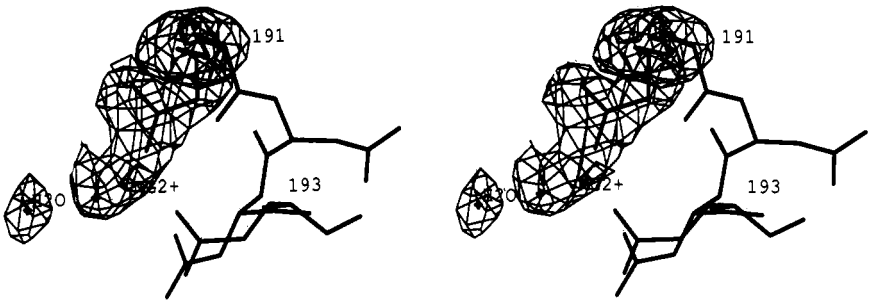

FIGURE 3: Parts of the final $|F_o| - |F_c|$ electron density map of the activated ternary complex of RuBP-carboxylase from *R. rubrum*. The activator site and its immediate surroundings are shown. The coordinates for the refined model of the ternary complex are superimposed. The contributions of the carbamylated side chain of Lys191, the Mg(II) ion, and the water molecule were not included in the structure factor calculation. The contour level is at 2.5 times the standard deviation of the electron density map.

refined to 1.7 Å, with which the new model had most atomic positions in common. The two subunits of the L_2 dimer are crystallographically independent and the structure determination therefore gives independent results for both subunits.[2] In the following, the results we describe are valid for both subunits unless otherwise stated.

The low pH at which the *R. rubrum* enzyme was crystallized effectively prevented any carbamylation of Lys191 (Schneider et al., 1986a). Fortunately, the increased solubility of the enzyme associated with higher pH can be compensated for by the addition of a precipitant to prevent the crystals from dissolving. In the presence of 50% MPD, the crystals still diffract under conditions that in solution would guarantee a high degree of activation (pH 8.1, 50 mM $MgCl_2$ and 25 mM $NaHCO_3$). This method of stabilizing crystals has earlier been used to study inhibitor binding to the deactivated form of the enzyme (Lundqvist & Schneider, 1989). It was shown that MPD neither binds to the active site nor interferes with inhibitor binding.

A simple trapping experiment, based on the method described by Badger and Lorimer (1981) was performed to qualitatively verify the presence of carbamate in the crystals (unpublished results). The experiment showed that the carbamate is formed in more than 60% of the protomers in the crystals. This estimate of the extent of carbamylation at Lys191 is probably too low, since trapping of this species is dependent on the speed with which the crystals dissolve and the complex with the inhibitor 2-CABP is formed. Another way to estimate the occupancy at the metal-binding site is by analysis of the refined temperature factors for the carbamate and Mg(II) ion. The temperature factors for these atoms are in the same range (approximately 25–34 Å^2) as the values of the surrounding amino acid side chains (Lys191, Asp193, and Glu194). From this, we can conclude that the occupancy of the carbamate and Mg^{2+} at the activator site of the enzyme is high and similar in both subunits.

An electron density map calculated with the coefficients $|F_o| - |F_c|$ revealed differences in electron density at the side chain of Lys191, the site of activation, and neighboring side chains. Figure 3 shows the electron density for the carbamylated lysine side chain and the Mg(II) ion after model building and crystallographic refinement. At the position of Lys191 in the native structure, there is continous electron density corresponding to the carbamylated lysine moiety.

Close to the carbamate oxygens there is electron density that we interpret as the magnesium ion bound to the carbamate. Since the number of electrons in a magnesium ion and a water molecule is very similar, these atoms cannot be distinguished crystallographically at the present resolution. The interpretation of this difference electron density as the bound Mg(II) is based on the following evidence. The Mg(II) ion is coordinated to the carboxyl groups of residues Asp193 and Glu194 and the carbamate. These are the same three enzyme ligands that are observed close to the metal ion in the spinach quaternary complex (Andersson et al., 1989). Superposition of the two structures places the metal ions close to each other (distance approximately 1.6 Å). Further evidence for the assignment of this electron density to Mg(II) is the flip of the Glu194 side chain, which in the nonactivated state interacts with Asn111, Lys168, and Asn112 while in the activated form it is positioned close to the Mg(II) ion as well as Lys168 and away from Asn111 and Asn112 of the N-terminal domain of the second subunit. The position of the Mg(II) ion is also very close to the binding site of heavy-metal derivatives such as Sm(III) or Gd(III), used in the structure determination of the native enzyme (Schneider et al., 1986b). Gd(III) has been shown to be able to form a stable quaternary complex with the spinach enzyme (Andrews & Lorimer, 1987).

Table II: Metal-Binding Site in RuBP-Carboxylase[a]

OF1 Lys191 (carbamylated)
OD1 Asp193
OE1 Glu194
ND2 or OD1 Asn111[b]
solvent

[a] Atoms closer than 3.5 Å to the Mg(II) ion in the model are included. [b] Only observed in the B-subunit.

One major difference in the metal-binding site between the two subunits is observed. While the Mg(II) ion in subunit A is coordinated to the protein ligands Asp193 and Glu194 and the carbamate, an additional protein side chain is found in the B-subunit within the first coordination sphere of the metal ion. The side chain of the conserved Asn111 is close to the Mg(II) ion. The difference in the metal coordination between the two subunits is probably due to the different conformation of the loop involving residues 109–115, connecting helix αC and strand βE of the N-terminal domain (Schneider et al., 1990a). In the A-subunit, the Asn side chain points away from the metal ion and interacts with the side chain of Lys168 and the main-chain oxygen of Thr106. But since the carbamate is formed and the metal ion is bound in the A-subunit as well, the Asn side chain does not seem to be important for the formation of the ternary complex. In the quaternary complex of the spinach enzyme with the reaction intermediate analogue 2-CABP (Andersson et al., 1989), this side chain interacts with the O4 oxygen of the inhibitor and is not liganded to the Mg(II) ion. Site-directed mutagenesis might help to define the role of this conserved residue in activation and catalysis.

[2] The two subunits have been labeled A and B, respectively. These labels refer to the chain identifiers that have been used in the atomic coordinate file, deposited with the Brookhaven Protein Data Bank.

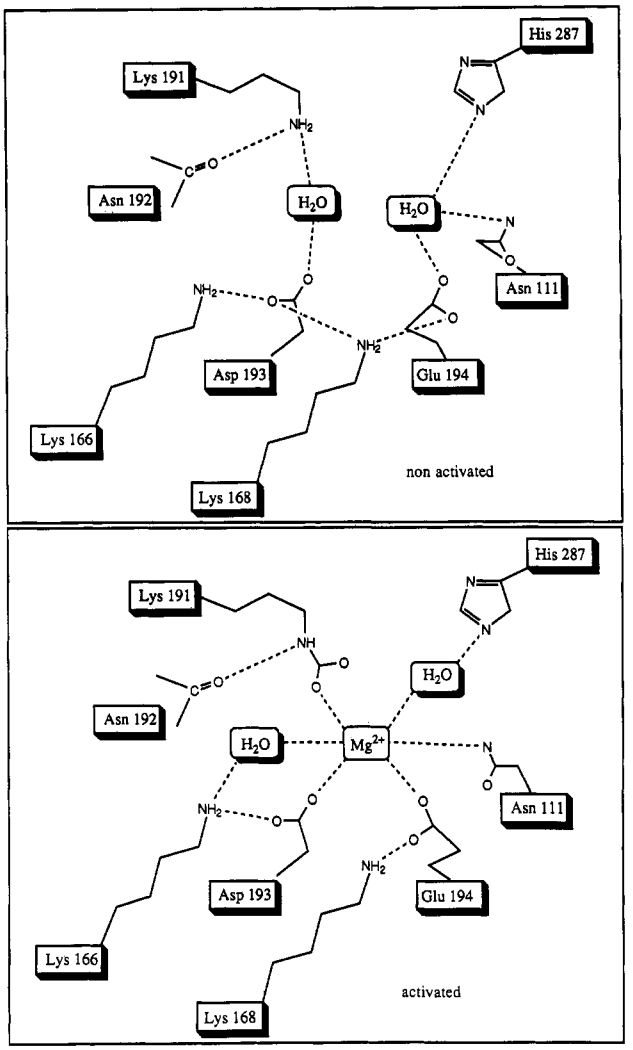

FIGURE 4: Schematic diagrams of the activator site in RuBP-carboxylase from *R. rubrum*. Possible hydrogen bonds are indicated by the dashed lines. Upper panel, nonactivated enzyme; lower panel, activated enzyme.

Electron density maps show one well-ordered water molecule coordinated to the metal and within hydrogen bonding distance to Lys166 (Figure 3). In Table II we list the residues found in the vicinity of the metal in our model. Figure 4 gives a more schematic view of the activator site and the hydrogen-bonding pattern in its immediate proximity in both activated and nonactivated RuBP-carboxylase. In none of the subunits do we observe octahedral coordination geometry around the Mg(II) ion. However, at the limited resolution of the electron density maps, it is not possible to exclude that one of the protein side chains might coordinate with both oxygen atoms to the metal. Furthermore, additional solvent molecules within the first coordination sphere of Mg(II) might not be ordered enough to be seen in our electron density maps.

Discussion

A conformational change upon activation of the enzyme has been invoked to explain differences observed between the two states of the enzyme in a number of experiments [for a summary see Andrews and Lorimer (1987)]. We cannot rule out that a conformational change has been prevented by crystal lattice forces. However, we have shown here that a carbamate can be formed and stabilized in the crystals without the occurrence of a large structural change. Furthermore, it is worth noticing the close similarity of the *R. rubrum* and the spinach carboxylase structures, even though they represent two very different forms of the enzyme. A comparison of the crystal structures of the nonactivated enzyme from *R. rubrum* and the spinach enzyme, crystallized in the activated form, failed to detect any large conformational changes as the result of activation (Schneider et al., 1990b). The assumption that the activation does not induce any major conformational changes is further supported by neutron scattering experiments (Donnely et al., 1984), which did not reveal any structural differences upon carbamylation.

Table III: Solvent Accessibilities at the Active-Site Lysine Residues[a]

residue no.	solvent accessibility (Å^2)
166A	31.6
166B	20.7
168A	1.8
168B	2.9

[a] Solvent accessibilities were calculated with an algorithm described by Lee and Richards (1971).

The ternary complex enzyme–CO_2–Mg(II) has been investigated by electron paramagnetic resonance (EPR) spectroscopy with Co(II) (Nilsson et al., 1984) and Cu(II) (Styring & Bränden, 1985). Spectra of the Co(II)-activated enzyme indicate that the coordination geometry of the metal ion is not greatly perturbed upon binding to the active site. EPR spectra of the enzyme-bound Cu(II) display a nitrogen hyperfine structure, and it has thus been suggested that at least one nitrogen atom is liganded to the Cu(II) ion. The crystallographic analysis has shown that, in fact, one nitrogen-containing amino acid side chain, Asn111, is close to the metal ion in the ternary complex. Crystallographically, we cannot at the present resolution of the electron density maps distinguish whether the oxygen or the nitrogen is coordinated to the Mg(II) ion. Furthermore, the side chain of His287 is close to the metal-binding site (approximately 4.5 Å). It is conceivable that in the complex with Cu(II), which has a higher preference for nitrogen ligands, this side chain might move into coordination distance, thus increasing the number of possible nitrogen ligands.

Trinitrobenzenesulfonate (TNBS), a group-selective reagent that is specific for reactions with unprotonated amines, has been used to probe the active site of RuBP-carboxylase (Hartman et al., 1985). In the case of the carbamylated enzyme from *R. rubrum*, Lys166 is the major target of arylation by TNBS, while in the noncarbamylated form there are several additional sites. The specificity of this reagent toward Lys166 in the activated *R. rubrum* enzyme allowed the pK_a values of this residue to be determined, and the observed pK_a (7.9) of Lys166 is very low. This low pK_a of Lys166 can be explained by its proximity to the side chain of Lys168 and to the metal ion in the activated form of the enzyme. However, Lys168 is almost equally close to the metal and there is no obvious reason why Lys168 should not have similar properties to Lys166, such as low pK_a and increased nucleophilicity. An accessible surface calculation shows that this residue is completely buried in the ternary complex (Table III), and a labeling reagent has no access to this residue. Steric hindrance thus might mask an increased reactivity for the Lys168 side chain.

The metal ion in RuBP-carboxylase has been implicated to be essential for proper orientation of the substrate (Lundqvist & Schneider, 1989) and polarization of the carbon–oxygen bond at C2 (Andrews & Lorimer, 1987). Carbamylation of Lys191 completely changes the microenvironment of the active site by replacing a positive charge with the negatively charged carbamate. This chemical modification in fact completes the metal-binding site. An understanding of the molecular

mechanism of activation, however, does not provide us with an answer to why the enzyme utilizes a carbamate for the activation process. In other words: why is RuBP-carboxylase not permanently activated? The dual role of CO_2, both as substrate and activator, might be involved in regulating the activity in vivo (Andrews & Lorimer, 1987). An interesting observation is that a functional metal-binding site can be built up by using only residues from β-strand and loop 2 of the β/α barrel. The usage of only one loop to provide the necessary ligands to the metal could give the advantage of a metal-binding site with high structural integrity, allowing the rest of the structure and bound intermediates to undergo structural changes without disrupting the metal binding. By retaining the same Cα positions of the loop, no other naturally occurring amino acid could play the structural role of the carbamate. They would either be too short or provide the wrong charge. Furthermore, there still remains the possibility that the carbamate may play a more active role during catalysis, CO_2 thus not only being a substrate but also acting as its own cofactor.

ACKNOWLEDGMENTS

We thank Drs. G. Lorimer and S. Gutteridge for gifts of the enzyme and Drs. I. Andersson, S. Knight, and C.-I. Bränden for access to the refined coordinates for spinach RuBP-carboxylase prior to publication.

Registry No. RuBP, 9027-23-0; L-Asp, 56-84-8; L-Glu, 56-86-0; L-Lys, 56-87-1; L-Asn, 70-47-3; Mg, 7439-95-4.

REFERENCES

Andersson, I., Knight, S., Schneider, G., Lindqvist, Y., Lundqvist, T., Brändén, C.-I., & Lorimer, G. (1989) *Nature 337*, 229–234.

Andrews, T. J., & Lorimer, G. H. (1987) in *The Biochemistry of Plants* (Hatch, M. D., Ed.) Vol. 10, pp 131–218, Academic Press, Orlando, FL.

Badger, M. R., & Lorimer, G. H. (1981) *Biochemistry 20*, 2219–2225.

Blum, M., Metcalf, P., Harrison, S. C., & Wiley, D. C. (1987) *J. Appl. Crystallogr. 20*, 235–242.

Bränden, R., Nillson, T., & Styring, S. (1984) *Biochemistry 23*, 4373–4378.

Brünger, T. A., Kuriyan, J., & Karplus, M. (1987) *Science 235*, 458–460.

Chapman, M. S., Suh, S. W., Curmi, P. M. G., Cascio, D., Smith, W. W., & Eisenberg, D. (1987) *Nature 329*, 354–356.

Chapman, M. S., Suh, S. W., Curmi, P. M. G., Cascio, D., Smith, W. W., & Eisenberg, D. (1988) *Science 241*, 71–74.

Christeller, J. T. (1981) *Biochem. J. 193*, 839–844.

Donnely, M. I., Hartman, F. C., & Ramakrishnan, V. (1984) *J. Biol. Chem. 259*, 406–411.

Durbin, R. M., Burns, R., Moulai, J., Metcalf, P., Freymann, D., Blum, M., Anderson, J. E., Harrison, S. C., & Wiley, D. C. (1986) *Science 232*, 1127–1132.

Estelle, M., Hanks, J., McIntosh, L., & Somerville, C. (1985) *J. Biol. Chem. 260*, 9523–9526.

Hardy, R. W. F., Havelka, U. D., & Quebedeaux, B. (1978) in *Photosynthetic Carbon Assimilation* (Siegelman, H. W., & Hind, G., Eds.) pp 165–178, Plenum, New York.

Hartman, F. C., Milanez, S., & Lee, E. H. (1985) *J. Biol. Chem. 260*, 13968–13975.

Jones, T. A. (1978) *J. Appl. Crystallogr. 11*, 268–272.

Jones, T. A. (1982) in *Computational Crystallography* (Sayre, D., Ed.) pp 303–317, Oxford University Press, New York.

Jones, T. A., Bergdoll, M., & Kjeldgaard, M. (1990) in *Molecular Modelling*, Springer Verlag, New York.

Knight, S., Andersson, I., & Bränden, C.-I. (1989) *Science 244*, 702–705.

Konnert, J. H., & Hendrickson, W. A. (1980) *Acta Crystallogr. A36*, 344–350.

Larimer, F. W., Lee, E. H., Mural, R. J., Machanoff, R., & Soper, T. S. (1987) *J. Biol. Chem. 262*, 15327–15329.

Lee, B., & Richards, F. M. (1971) *J. Mol. Biol. 55*, 379–400.

Lorimer, G. H. (1979) *J. Biol. Chem. 254*, 5599–5601.

Lorimer, G. H. (1981) *Biochemistry 20*, 1236–1240.

Lorimer, G. H., & Miziorko, H. M. (1980) *Biochemistry 19*, 5321–5328.

Lorimer, G. H., Gutteridge, S., & Madden, M. W. (1987) in *Plant Molecular Biology* (von Wettstein, D., & Chua, N.-H., Eds.) pp 21–31, Plenum Press, New York.

Lundqvist, T., & Schneider, G. (1989) *J. Biol. Chem. 264*, 7078–7083.

Nargang, F., McIntosh, L., & Somerville, C. (1984) *Mol. Gen. Genet. 193*, 220–224.

Nilsson, T., Bränden, R., & Styring, S. (1984) *Biochim. Biophys. Acta 788*, 274–280.

Pierce, J., & Gutteridge, S. (1985) *Appl. Environ. Microbiol. 49*, 1094–1100.

Pierce, J., & Reddy, G. S. (1986) *Arch. Biochem. Biophys. 245*, 483–493.

Robison, P. D., Martin, M. N., & Tabita, F. R. (1979) *Biochemistry 18*, 4453–4458.

Schneider, G., Bränden, C.-I., & Lorimer, G. (1986a) *J. Mol. Biol. 187*, 141–143.

Schneider, G., Lindqvist, Y., Brändén, C.-I., & Lorimer, G., (1986b) *EMBO J. 5*, 3409–3415.

Schneider, G., Lindqvist, Y., & Lundqvist, T. (1990a) *J. Mol. Biol. 211*, 989–1008.

Schneider, G., Knight, S., Andersson, I., Brändén, C.-I., Lindqvist, Y., & Lundqvist, T. (1990b) *EMBO J. 9*, 2045–2050.

Somerville, C. R., & Somerville, S. (1984) *Mol. Gen. Genet. 193*, 214–219.

Steigemann, W. (1974) Ph.D. Thesis, Technische Universitat Munchen.

Styring, S., & Bränden, R. (1985) *Biochemistry 24*, 6011–6019.